CBX 04-46
January 13, 2005
Feng Liu
Yongsheng Gao

Update on Exclusive D^0 Semileptonic Decays

Abstract

This is an update on the results for ICHEP'04 with improved MC based on a data sample of 57.2 pb^{-1} collected at the $\psi(3770)$ resonance, we have presented improved measurements of absolute branching ratios for D^0 semileptonic decays into $K^-e^+\nu$, $\pi^-e^+\nu$, $K^{*-}e^+\nu$ and the first observation and measurement of $D^0 \to \rho^-e^+\nu$.

Contents

1 Introduction

In the Standard Model of electroweak interactions, the quark mixing is conventionally expressed by the Cabibbo-Kobayashi-Maskawa (CKM) matrix:

$$\begin{pmatrix} d' \\ s' \\ b' \end{pmatrix} = \begin{pmatrix} V_{ud} & V_{us} & V_{ub} \\ V_{cd} & V_{cs} & V_{cb} \\ V_{td} & V_{ts} & V_{tb} \end{pmatrix} \begin{pmatrix} d \\ s \\ b \end{pmatrix} \tag{1}$$

CP symmetry violation is an expected consequence of the Standard Model with three quark generations which incorporates a complex phase in the CKM quark-mixing matrix. The Standard Model predicts a multitude of CP violating effects in B decays which have been observed at B factories BABAR and BELLE. To test the predictions of the Standard Model, we need to measure the CKM elements as precisely as possible.

In principle, the values of the CKM matrix elements can be determined from weak decays of the relevant quarks. The current precision for V_{cs} and V_{cd} is 13% and 7% respectively [1]. At CLEO-c, D meson semileptonic decays can be used to determine two CKM elements V_{cs} and V_{cd} more precisely.

In the Standard Model, the semileptonic charm meson decay matrix element can be expressed as

$$\mathcal{M} = \frac{G_F}{\sqrt{2}} V_{cq'} \bar{u}(q_\nu) \gamma^\mu (1 - \gamma_5) u(q_\ell) J^\mu, \tag{2}$$

where G_F is the Fermi coupling constant, $V_{cq'}$ is a CKM matrix element; q_ν and q_ℓ are the four-momenta of the neutrino and the lepton, respectively; $J^\mu \equiv \langle \text{hadrons} | V^\mu - A^\mu | 0 \rangle$ is the hadronic current, and V^μ and A^μ are the vector and axial vector quark currents.

The differential decay rate for $D \to P\ell\nu$ with the electron mass effects neglected (P stands for a pseudoscalar meson) can be expressed as [2]:

$$\frac{d\Gamma}{dq^2} = \frac{G_F^2}{24\pi^3} |V_{cq'}|^2 p_P^3 \left| f_+(q^2) \right|^2, \tag{3}$$

where q^2 is the four-momentum transfer squared between the parent D meson and the final state meson, p_P is the momentum of the pseudoscalar meson in the D rest frame, and $V_{cq'}$ is the relevant CKM matrix element in $c \to q'$ transition, either V_{cs} or V_{cd}. $f_+(q^2)$ is the form factor which measures the probability that the flavor changed quark ($c \to q'$) and the spectator quark ($\bar{q}$) will form a meson in the final state. The corresponding branching fractions can be obtained from

$$\mathcal{B}(D \to P\ell\nu) = \tau_D \times \int_{q^2} dq^2 \frac{d\Gamma}{dq^2}. \tag{4}$$

From the measurements of the branching fractions, we can extract the CKM elements V_{cs} and V_{cd}. To dertermine an individual matrix element, theory must provide the absolute normalization of the form factor describing the decay at some fixed q^2 point, usually at $q^2 = 0$. Since theory also provide the q^2 dependence of the form factor, we can check the theory by measuring the form factor shape. At CLEO-c, the gold-plated modes for the determinations of V_{cs} and V_{cd} are the decays $D^0 \to K^- e^+ \nu$ and $D^0 \to \pi^- e^+ \nu$, respectively.

Form factors in charm semeleptonic decays play an important role in testing lattice QCD and testing other theories of heavy quark decays. The form factors in charm semileptonic decays are related to those in B decays by Heavy Quark Symmetry and so aid the determination of V_{ub} which is hard to be determined precisely at B factories due to the small branching fractions for $b \to u$ transitions and huge backgrounds from $b \to c$ transitions.

The shape of the form factors governing semeleptonic decays have not been well-measured. At CLEO-c, the kinematics of the threshold production allow for the isolation of the background free samples of semileptonic decays. This in turn allows measurements of the form factors with much better signal to background ratios.

Compared to leptonic decays, semileptonic decays have two distinct advantages. First, they have substantially larger braching fractions and cleaner signatures; and second, they offer more observables, overall rate and form factors, while leptonic decays manifest rate only. Taking advantage of the latter feacture, one can use inclusive semileptonic decays to test the heavy quark expansion theory, HQET, and exclusive semileptonic decays to test Lattice QCD.

2 Analysis Technique for D Semileptonic Decays

2.1 Analysis Technique

We fully reconstruct one D meson of the $D\bar{D}$ pairs in the events produced at the $\psi(3770)$ resonance which helps determine the charge and flavor of the semileptonic decay of the other D meson if available, resulting in great suppression of the backgrounds. The fully reconstructed D meson serves as a tag. We identify an electron and a set of hadrons recoiling against the tag, reconstructing the missing momentum and missing energy. The excellent particle identification of the CLEO-c dectector are well-suited for this purpose. The unique kinematics of threshold

production provide additional and very powerful means to reject background from misidentified and missing particles. The difference between the missing energy and missing momentum in a event $U = E_{miss} - p_{miss}$ will peak at zero if the event is correctly reconstructed due to the undetected neutrino.

2.2 Absolute Branching Fraction Measurements

To measure the absolute D semileptonic decay branching fractions $\mathcal{B}$, we use D meson hadronic decays $D^0 \to K^-\pi^+$, $K^-\pi^+\pi^0$, $K^-\pi^+\pi^0\pi^0$, $K^-\pi^+\pi^+\pi^-$, $K_S\pi^+\pi^-$, $K_S\pi^+\pi^-\pi^0$, $K_S\pi^0$, $\pi^+\pi^-\pi^0$, and K^-K^+ to tag the other $\bar{D}^0$ semileptonic decays (signal). The number of tag yield and signal yield for semileptonic decays are given by:

$$\begin{aligned} N_{tag} &= 2N_{D\bar{D}}\epsilon_{tag}\mathcal{B}_{tag}, \\ N_{signal} &= 2N_{D\bar{D}}\mathcal{B}\epsilon_{signal}\mathcal{B}_{tag}. \end{aligned} \tag{5}$$

Here $N_{D\bar{D}}$ is the number of $D\bar{D}$ pairs produced at the $\psi(3770)$ resonance, N_{signal} and N_{tag} are the number of the signal and tag events observed, ϵ_{signal} and ϵ_{tag} are the efficiencies for the signal and tag events. The efficiency for the signal events ϵ_{signal} is obtained for fully constructed tag D and the other $\bar{D}$ semileptonic decays, ie, it includes the tag side. The branching fraction can be obtained:

$$\mathcal{B} = \frac{N_{signal}/\epsilon_{signal}}{N_{tag}/\epsilon_{tag}} = \frac{N_{signal}}{N_{tag} \times \frac{\epsilon_{signal}}{\epsilon_{tag}}} \tag{6}$$

Therefore the ratio $\epsilon \equiv \epsilon_{signal}/\epsilon_{tag}$ gives the efficiency of reconstructing one $\bar{D}^0$ semileptonic decay in presence of a tag D^0.

3 Event Selection

3.1 Minor changes after ICHEP

Since it is well-established that dE/dx provides 4σ kaon and pion separation at 0.7 GeV/c from Gocha's study, we increase the minimum momentum for RICH particle identification cut from 0.55 GeV/c to 0.7 GeV/c for the charged kaon or pion from the D^0 semileptonic decays.

Another minor change after ICHEP, we now apply mode-dependent ΔE cuts which will be discussed later.

3.2 Major change after ICHEP

The major change after ICHEP is that many bugs have been found in the MC samples used for ICHEP and now fixed. The main efforts after ICHEP'04 is to re-generate signal MC samples

and generic MC samples. We now generate larger signal MC samples for the signal efficiencies and 10 times luminosity gerenic $D\bar{D}$ MC sample for tag efficiencies, background and systematics studies using the release with all known bugs fixed. With these new MC samples, we expect the systematics can be improved compared to the results for ICHEP'04. While for continuum and radiative return $\psi(2S)$ backgrounds, we still used the MC samples for ICHEP. In our analysis, these backgrounds are too tiny and negligible.

3.3 Event Selection for the Tag D's

For completeness, the criteria for hadrons from the tag D decays are listed below [3].

- Hadrons from Tagging D's:
  - ◇ Good track:
    - ▷ $|d_0|$ <0.005m, $|z_0| < 0.05$m, $|\cos\theta| < 0.93$, $0.05 < p < 2$ GeV;
    - ▷ hitfraction>0.5;
  - ◇ Lepton veto: only for the events with two tracks and no showers with $E_\gamma > 50$ MeV on the other side (DTagUtilities) which help to reject some cosmic backgrounds;
  - ◇ Hadron ID:
    - ▷ $3|\sigma|$ dE/dx for kaons and pions;
      for $p > 0.55$ GeV, $LL_\pi - LL_K + \sigma_\pi^2 - \sigma_K^2 > (<)0$ and $N^\gamma_{K(\pi)} > 2$ for K(π) within $|\cos\theta| \leq 0.8$ if RICH available; otherwise, $\sigma_\pi^2 - \sigma_K^2 > (<)0$ for kaons and pions;
- π^0 and showers:
  - ◇ Good showers: noTrackMatch(), !hot(), $E_\gamma > 30$ MeV;
  - ◇ π^0: two good showers (default $E9/E25$ cut) within $(-3.0, 3.0)\sigma$ and contrained to the π^0 mass m_{π^0};
- K^0_S:
  - ◇ within 12 MeV of its nominal mass;

For flavored tag modes, we separate D^0 and $\bar{D}^0$ tags, we use minimum $|\Delta E|$ to select one candidate per tag mode per flavor to avoid double counting. For each unflavored tag mode, if there are more than one candidates, we further check whether these candidates will build a double tag event. If they do, we choose the $D^0\bar{D}^0$ pair with the average beam constrained mass ($(m_{bc1} + m_{bc2})/2$) closest to the D^0 normial mass as the Dhadron Group did [4]. If there is no double tag candidate in a event, we use the minimum ΔE to select one candidate per mode. The advantage of this procedure is that both flavored and unflavored tag modes are treated in the same way now. In

case of cross feeds among different tags, we have no way to justify which one should be chosen, so we keep all. The cross feeds among different tags will cancel in the branching fractions.

Since ΔE resolutions vary among different tag modes, we apply mode-dependent ΔE cuts. We use about 4σ ΔE for for $D^0 \to K^-\pi^+$, $K^-\pi^+\pi^0$, $K^-\pi^+\pi^+\pi^-$, $K_S\pi^+\pi^-$, $K_S\pi^0$ and K^-K^+, and about 3σ ΔE cuts for $D^0 \to K^-\pi^+\pi^0\pi^0$, $K_S\pi^+\pi^-\pi^0$ and $\pi^-\pi^+\pi^0$ with higher backgrounds. In Fig. 1, we present the fits to the ΔE for each tag mode with a double Gaussian for signals plus a 2^{nd} order polynomial for backgrounds. The ΔE cuts used are (-30, 30), (-50, 44), (-45, 35), (-20, 20), (-25, 25), (-45, 35), (-65, 55), (-46, 40) and (-23, 23) MeV for $D^0 \to K^-\pi^+$, $K^-\pi^+\pi^0$, $K^-\pi^+\pi^0\pi^0$, $K^-\pi^+\pi^+\pi^-$, $K_S\pi^+\pi^-$, $K_S\pi^+\pi^-\pi^0$, $K_S\pi^0$, $\pi^-\pi^+\pi^0$ and K^-K^+, respectively.

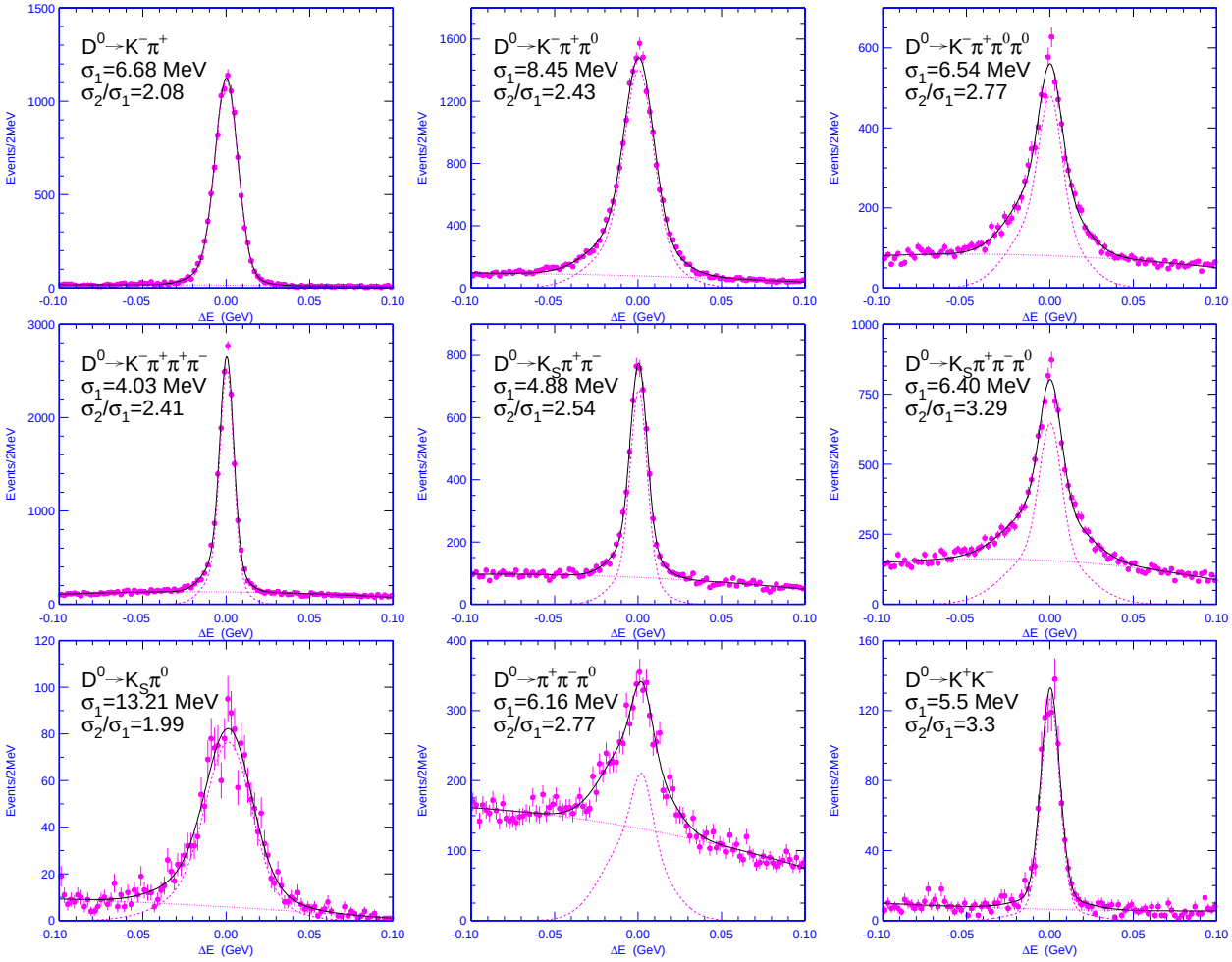

Figure 1: Fits to the ΔE for different tags with a double Gaussian for signals plus a 2^{nd} order polynomial for backgrounds.

In Fig. 2, we present the fits to the D^0 beam constrained masses in the data with a Gaussian and a bifurcated Gaussian to account for the initial state radiation (ISR) for signal plus Argus function for backgrounds. When fitting the beam constrained masses, we let the E_{beam} float. Similarly, we fit the D^0 beam constrained masses in the MC samples to obtain the tagging efficiencies with the cross-feed decays excluded, for example, $D^0 \to K_S\pi^0 \to \pi^+\pi^-\pi^0$ and $D^0 \to \pi^-\pi^+\pi^0$, $D^0 \to \pi^+\pi^+\pi^-\pi^-$ and $D^0 \to K_S\pi^+\pi^- \to \pi^+\pi^+\pi^-\pi^-$, $D^0 \to K_S\pi^+\pi^-\pi^0 \to \pi^+\pi^+\pi^-\pi^-\pi^0$ and $D^0 \to \pi^+\pi^+\pi^-\pi^-\pi^0$, and $D^0 \to K^-\pi^+\pi^+\pi^-$ and $D^0 \to K^-K_S\pi^+ \to K^-\pi^+\pi^+\pi^-$. While in the data, the cross-feeds cancel in the branching ratios (see Eq. 6) since it apprears in both N_{signal} and N_{tag}. The tag yields and tag efficiencies are given in Table 1. For the D^0 semileptonic decays, the selection criteria for the tag side will be the same throughout this analysis.

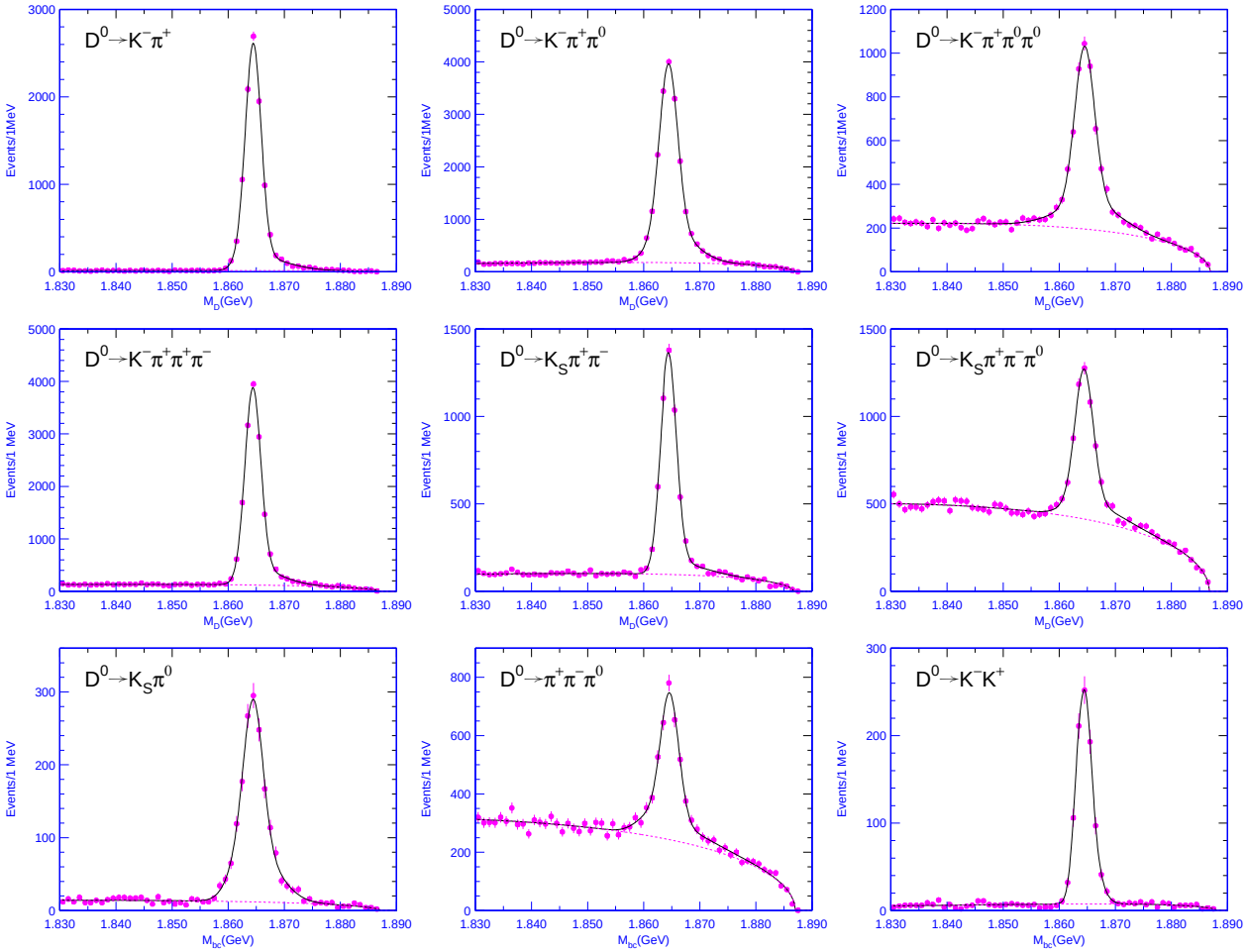

Figure 2: Fits to the beam constrained masses for different tags with a Gaussian and a bifurcated Gaussian to account for the initial state radiation for signals plus Argus function for backgrounds.

Table 1: The tag yields and efficiencies.

Tags:	tag yields	ϵ_{tag} (%)
$D^0 \to K^-\pi^+$	10223 ± 109	66.04 ± 0.12
$D^0 \to K^-\pi^+\pi^0$	18574 ± 173	33.24 ± 0.06
$D^0 \to K^-\pi^+\pi^0\pi^0$	4813 ± 229	15.92 ± 0.06
$D^0 \to K^-\pi^+\pi^+\pi^-$	14767 ± 145	44.45 ± 0.09
$D^0 \to K_S\pi^+\pi^-$	4879 ± 99	38.16 ± 0.15
$D^0 \to K_S\pi^+\pi^-\pi^0$	4299 ± 195	18.39 ± 0.09
$D^0 \to K_S\pi^0$	1585 ± 49	32.53 ± 0.23
$D^0 \to \pi^-\pi^+\pi^0$	2750 ± 146	41.23 ± 0.19
$D^0 \to K^-K^+$	901 ± 32	56.23 ± 0.37
all tags	62791±433	

3.4 Event Selection for D^0 Semileptonic Decays

One advantage of the threshold production is that kinematics provide very powerful means to reject background from misidentified and missing particles. As discussed in CBX-04-22 [5], we don't need tight hadron identification from the D^0 semileptonic decays. Besides the track quality requirements which are the same as those for tag D's, the following criteria apply to the D^0 semileptonic decays.

- Hadron ID for hadrons from D semileptonic decays
  - $\diamond$ $3|\sigma|$ dE/dx for kaons and pions;
    for $p > 0.7$ GeV, $LL_\pi - LL_K + \sigma_\pi^2 - \sigma_K^2 > (<)0$ for K(π) within $|\cos\theta| < 0.8$ if RICH available (without cut on $N^\gamma_{K(\pi)}$); otherwise, $\sigma_\pi^2 - \sigma_K^2 > (<)0$ dE/dx for kaons and pions;
- Electron ID: the electron ID package, based on E/p, dE/dx and RICH PDF, by Rochester group is used. The following cut applies
  - $\diamond$ $\mathcal{F}_{with-rich} > 0.8$ with $p_e > 0.2$ GeV/c (see Chulsu's writeup);
- π^0 and showers:
  - $\diamond$ Good showers: noTrackMatch(), !hot(), $E_\gamma > 30(50)$ MeV if in the good barrel (end-cap), SplitOff info. used;
  - $\diamond$ π^0: two good showers (default $E9/E25$ cut), at least one in the good barrel within $(-3.5, 3.0)\sigma$ and contrained to the π^0 mass m_{π^0};

- K_S: the K_S selection is the same as that for the tag D^0.

- Bremsstrahlung recovery: we recover the radiative photons from the electron candidate which satisfy the following criteria:

  - ◇ good showers with $E_\gamma > 10$ MeV and the angle $\theta_{e,\gamma}$ between the electron and showers less than 5^0 ($\theta_{e,\gamma} < 5^0$). It helps recover about 5% efficiency within $3\sigma_U$.

- Veto on extra track and shower: we used double D-tag to study the extra track in a double-D tagged events and found that the exrta track is well-modeled in MC, while the extra shower is not. So we don't allow any extra good track. We don't apply any cut on extra shower.

- For the semileptonic D decays, besides its direction constrained by $\hat{\mathbf{p}}_{semi} = -\hat{\mathbf{p}}_{tag}$, we further constrain its energy and momentum to be $E_{cm}/2.0$ and $\sqrt{(E_{cm}/2)^2 - 1.8645^2}$ in the $\psi(3770)$ rest frame to improve the resolution of U. For the tag D's, we apply mode-dependent ΔE cuts and require the beam constrained masses to be within $M_{bc} \in [1.858, 1.874]$ GeV. In case of multiple candidates due to the tag D^0, we choose the candidate with the minimum $|\Delta E|$.

3.5 Determination of Signal Yields

To determine the signal yields, we fit the U distributions with a Gaussian and Crystall Ball function [6] for signal. The Crystall Ball function has a core Gaussian with a power-law tail which is used to model the U distributions due to final state radiation. The shape of backgrounds is determined from 10 times generic MC sample, while its normalization is allowed to float.

4 Results for $D^0 \to K^- e^+ \nu$

In Fig. 3, we present the comparison of the distributions of $U = E_{miss} - p_{miss}$ for the selected $D^0 \to K^- e^+ \nu$ events between the data and MC using different tag modes. The comparison shows good agreement between the data and MC.

In Fig. 4, we present the missing mass squared for the selected $D^0 \to K^- e^+ \nu$ events, it peaks at zero due to the undetected neutrino. It means we do have neutrinos in the selected events.

In Fig. 5, we decompose different components using MC tags. For $D^0 \to K^- e^+ \nu$, there is considerable background from $D^0 \to K^{*-} e^+ \nu$ although its contribution is not significant. The fit to the backgrounds with a modified hyperbolic tanh(x) is also presented.

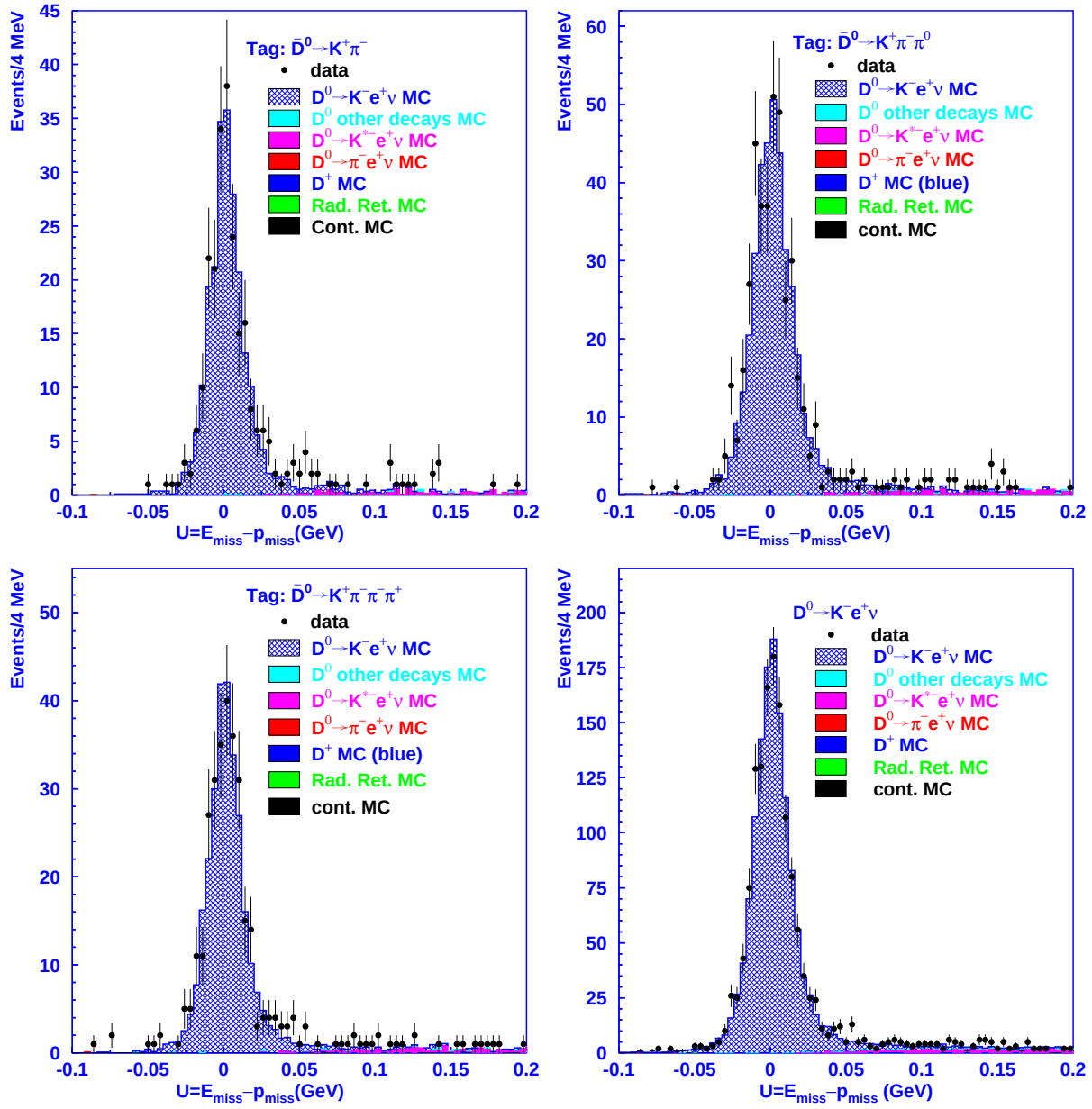

Figure 3: Comparison of $U = E_{miss} - p_{miss}$ for $D^0 \to K^-e^+\nu$ between the data and MC using the tags $\bar{D}^0 \to K^+\pi^-$, $K^+\pi^-\pi^0$, $K^+\pi^-\pi^-\pi^+$ and all tags combined with the branching fractions scaled by the new measured values.

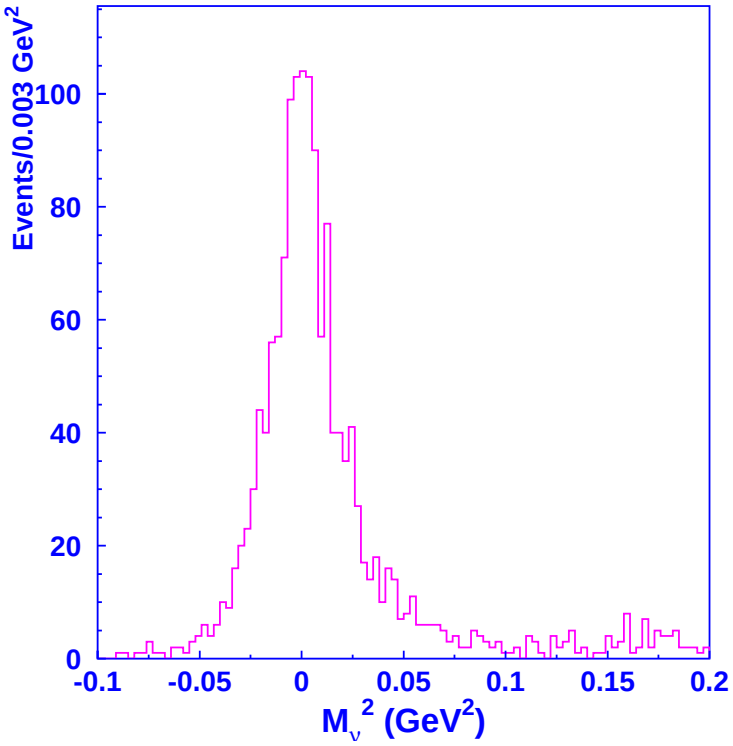

Figure 4: The missing mass squared of the selected $D^0 \to K^- e^+ \nu$ events. It peaks at zero due to the undetected neutrino.

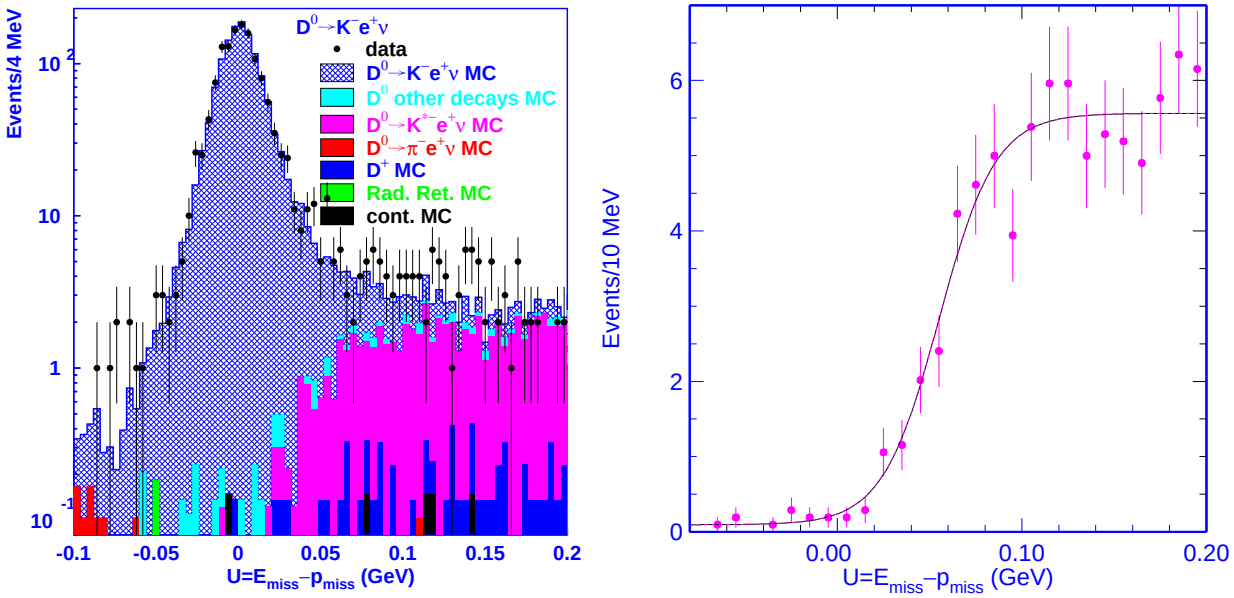

Figure 5: Background for $D^0 \to K^- e^+ \nu$ (left), the dominant backgroud comes from $D^0 \to K^{*-} e^+ \nu$ due to the mising π^0. The fit to the background with a modified hyperbolic tanh(x) function (right plot).

In Figs. 6 and 7, we present the fits to the U distributions for the selected $D^0 \to K^- e^+ \nu$ events with a Gaussian and a Crystal Ball function [6] for the signals to account for the tails due to the final state radiation of electron, and background described above with its shape fixed at the MC level, while its normalization is allowed to float. We fix parameters n and α determined from the fits to the signal MC samples. Our comparison (see Fig. 3) shows that the background is well-modeled in MC although we will consider its contribution to systematics later. The yields are given in Table 1. The efficiencies and branching fractions are also listed in Table 1 for different tag modes. The inclusions of the tails in the fits help increase about 5% efficiencies.

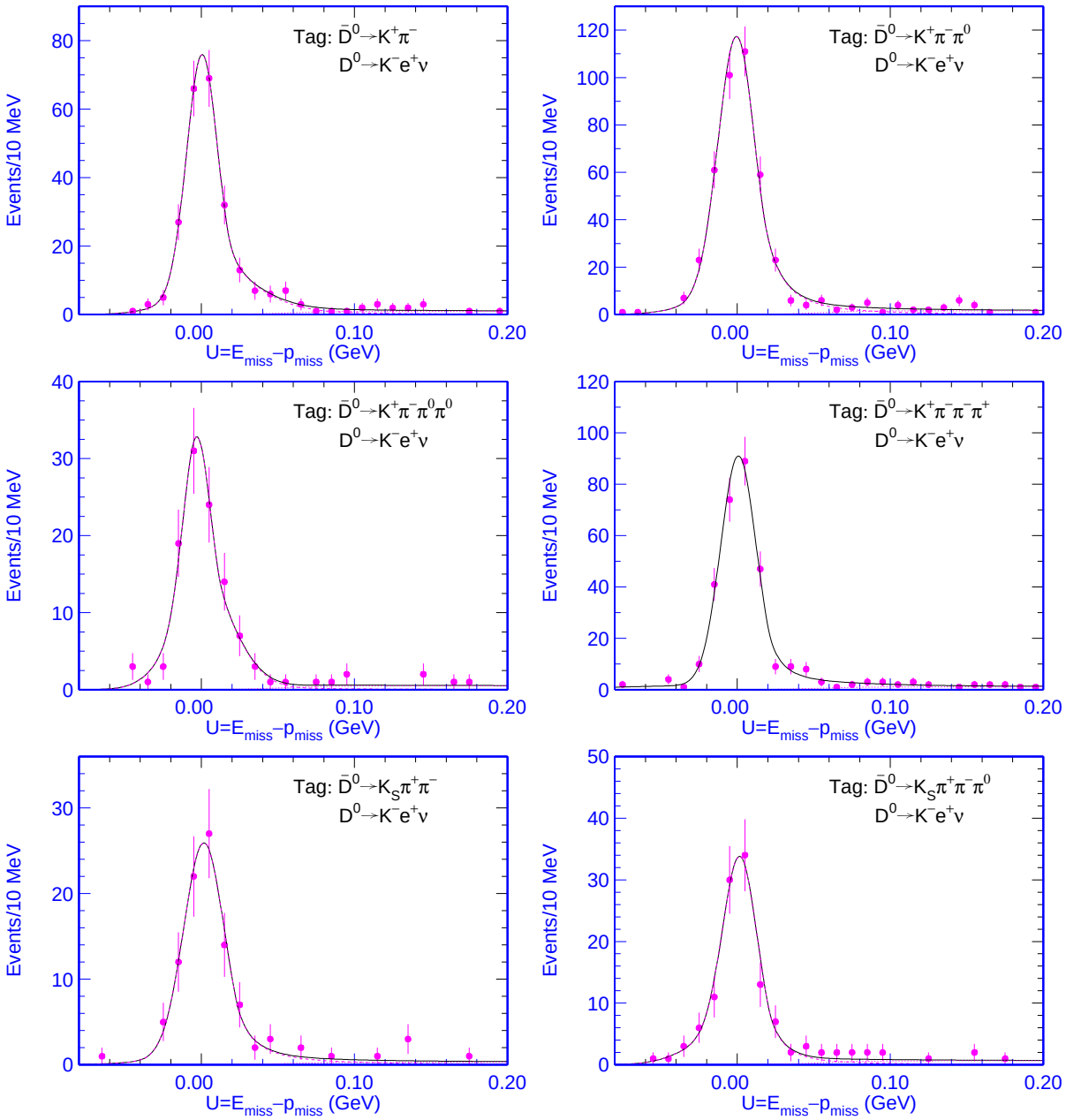

Figure 6: Fits to the U distributions for $D^0 \to K^- e^+ \nu$ using different tag modes.

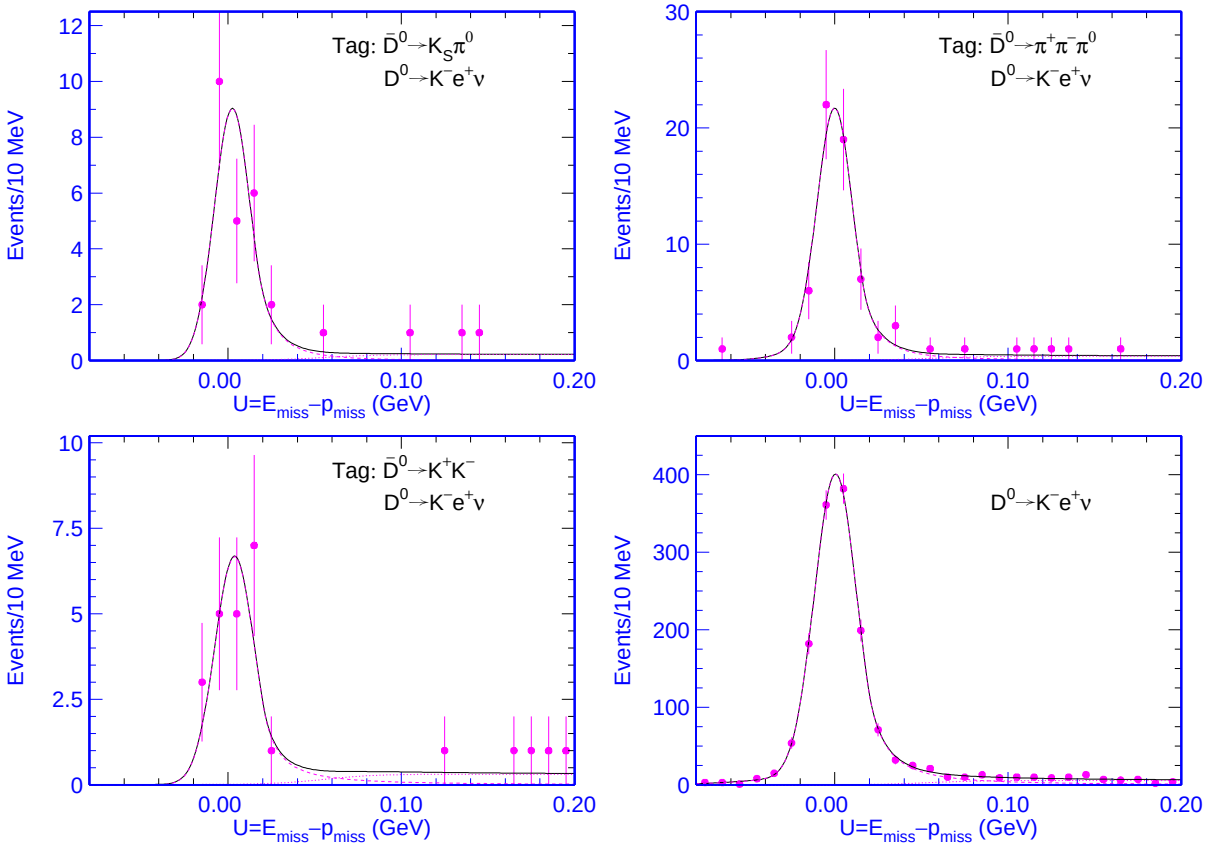

Figure 7: Fits to the U distributions for $D^0 \to K^-e^+\nu$ using different tag modes.

5 Results for $D^0 \to \pi^- e^+ \nu$

In Fig. 8, we present the $U = E_{miss} - p_{miss}$ distribution for the selected $D^0 \to \pi^- e^+ \nu$ events with all tag modes combined due to limited statistics. The comparison shows good agreement between the data and MC. The components of the backgrounds are decomposed and overlaid. The fit to the background with a Gaussian (dominant background from $D^0 \to K^- e^+ \nu$) plus a 2nd order polynomials is shown in Fig. 9a. We fit the U distribution with a Gaussian and Crystal Ball function (signal, near zero) and a Gaussian (the dominant $D^0 \to K^- e^+ \nu$ background) plus a 2nd order polynomials. The shape of backgrounds is fixed at the MC level, while its normalization is let to float when fitting. The signal yield, efficiencies and branching fraction are given in Table 2.

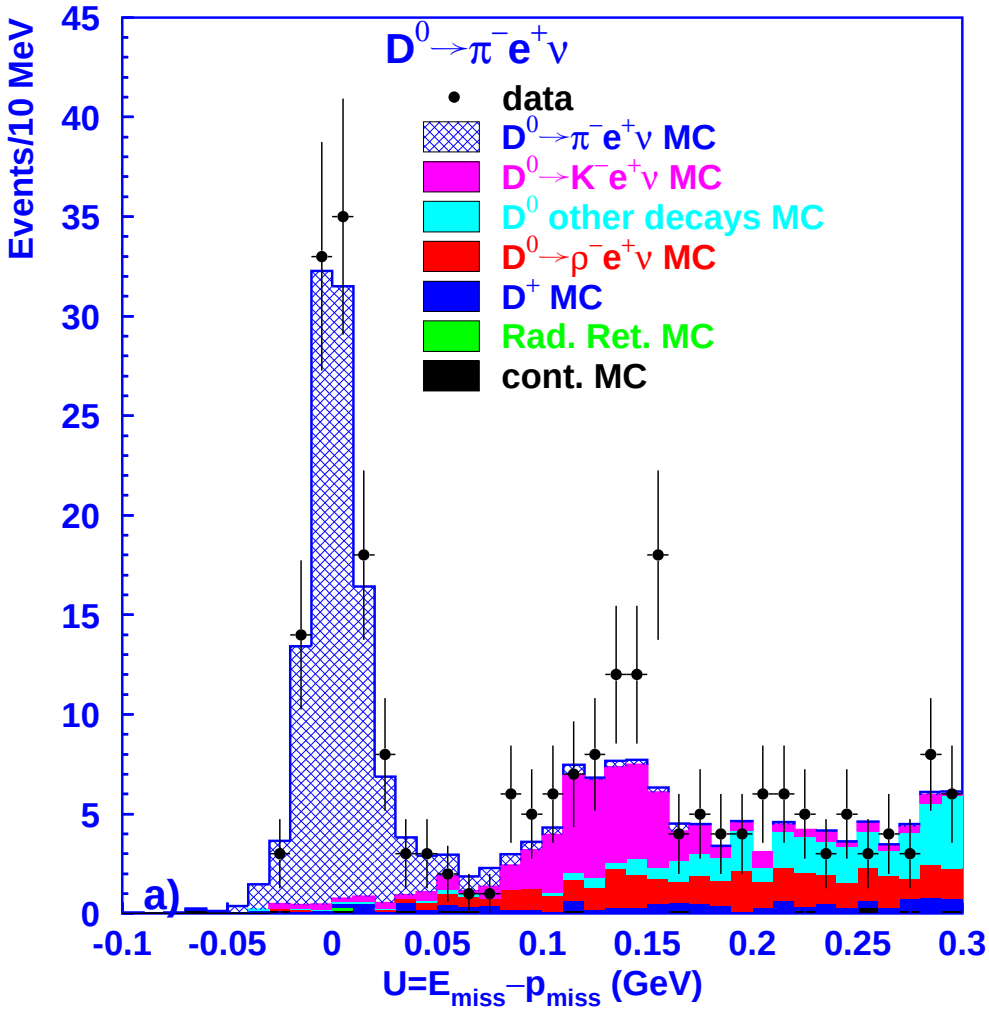

Figure 8: $U = E_{miss} - p_{miss}$ for the selected $D^0 \to \pi^- e^+ \nu$ events and the background components.

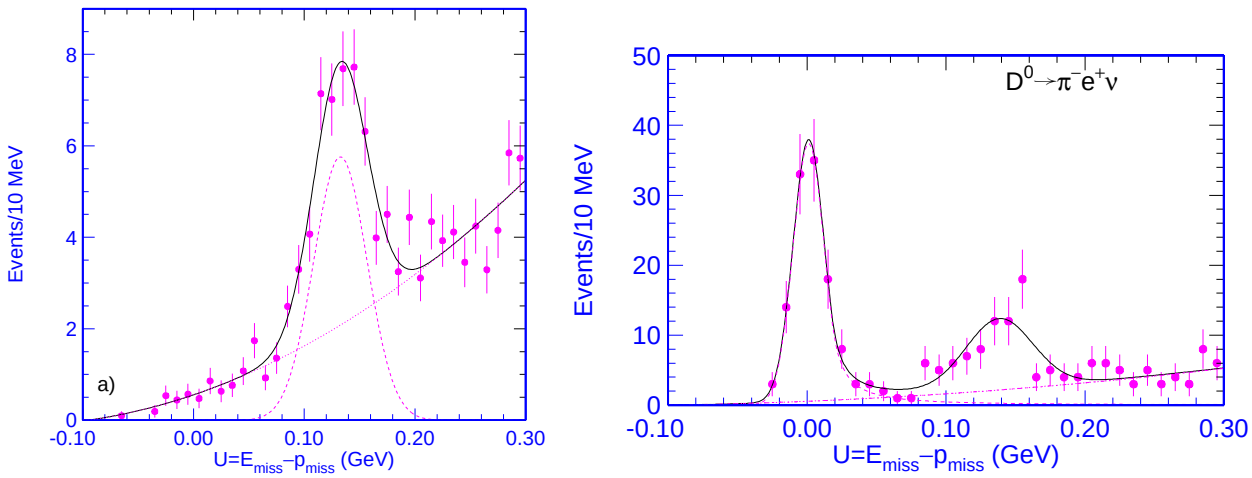

Figure 9: Fit to the backgrounds and fit to the U distribution for $D^0 \to \pi^- e^+ \nu$, see text.

6 $D^0 \to K^{*-} e^+ \nu$ and $D^0 \to \rho^- e^+ \nu$

- K^{*-} with $K^{*-} \to K^- \pi^0$ and $K^{*-} \to K_S \pi^-$ and $\rho^- (\to \pi^- \pi^0)$ selection:
  - ◇ the criteria for charged kaon and pion are the same as those from $D^0 \to K^- e^+ \nu$ and $D^0 \to \pi^- e^+ \nu$, π^0 selection is described in Sect. 3.4;
  - ◇ K^{*-}: we require the K^{*-} candidate to be within 100 MeV of its nominal mass. For the decay $K^{*-} \to K^- \pi^0$, the K^{*-} candidate with the smallest $\frac{(M_{K^*} - M_{K^*}^{PDG})^2}{\Gamma_{K^*}^2} + \frac{(M_{\pi^0} - M_{\pi^0}^{PDG})^2}{\sigma_{\pi^0}^2}$ is selected in case of multiple K^{*-} candidates. For the decay $K^{*-} \to K_S \pi^-$, the K_S selection is the same as that for the tag D^0.
  - ◇ ρ^-: we require the ρ^- candidate to be within 150 MeV of its nominal mass, the ρ candidate with the smallest $\frac{(M_\rho - M_\rho^{PDG})^2}{\Gamma_\rho^2} + \frac{(M_{\pi^0} - M_{\pi^0}^{PDG})^2}{\sigma_{\pi^0}^2}$ is selected in case of multiple candidates.

6.1 Results for $D^0 \to K^{*-} e^+ \nu$

In Fig. 10, we present the comparison for $D^0 \to K^{*-} e^+ \nu$ between the data and MC with different contributions superimposed. Fig. 11a shows the fit to the backgrounds for $D^0 \to K^{*-}(K^- \pi^0) e^+ \nu$ with a Gaussian for peaking backgrounds and a modified hyperbolic tanh(x) plus a 2^{nd} polynomial for non-peaking backgrounds. Fig. 11b shows the fit to the U distribution for the selected $D^0 \to K^{*-} e^+ \nu$ events where $K^{*-} \to K^- \pi^0$ with a Gaussian and Crystall Ball function for signal and backgrounds discribed above, the shape of backgrounds is fixed at the MC level, its normalization is allowed to float. The yield and efficiencies are given in Table 2.

In Fig. 12, we present the fit to the backgrounds for $D^0 \to K^{*-} e^+ \nu$ where $K^{*-} \to K_S \pi^-$ with a 3^{rd} order polynomial. We fit the U distribution with a Gaussian and Crystall Ball function for

signal and a 3^{rd} order polynomial for backgrounds, the shape of the backgrounds is fixed from MC and its normalization is allowed to float. The yield and efficiencies are given in Table 2.

We also model the backgrounds with a Fermi function for the above two modes $D^0 \to K^{*-}e^+\nu$, the fits give consistent signal yields.

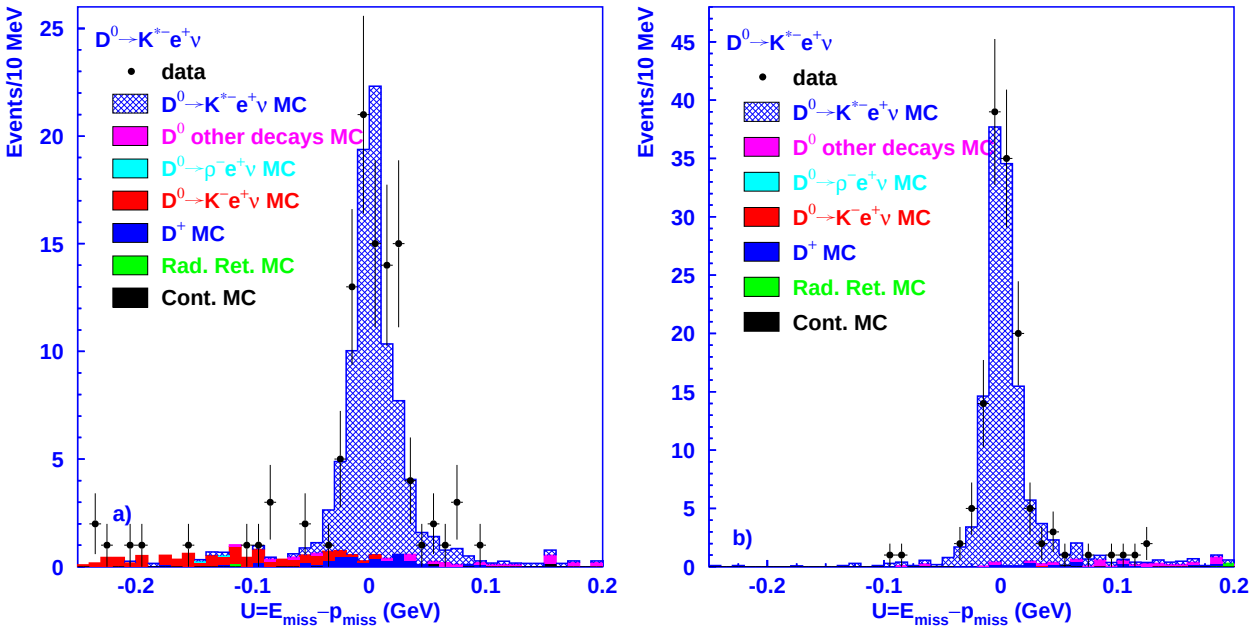

Figure 10: U distribution for the selected $D^0 \to K^{*-}e^+\nu$ events with $K^{*-} \to K^-\pi^0$ (left) and $K^{*-} \to K_S\pi^-$ (right) and the components of backgrounds.

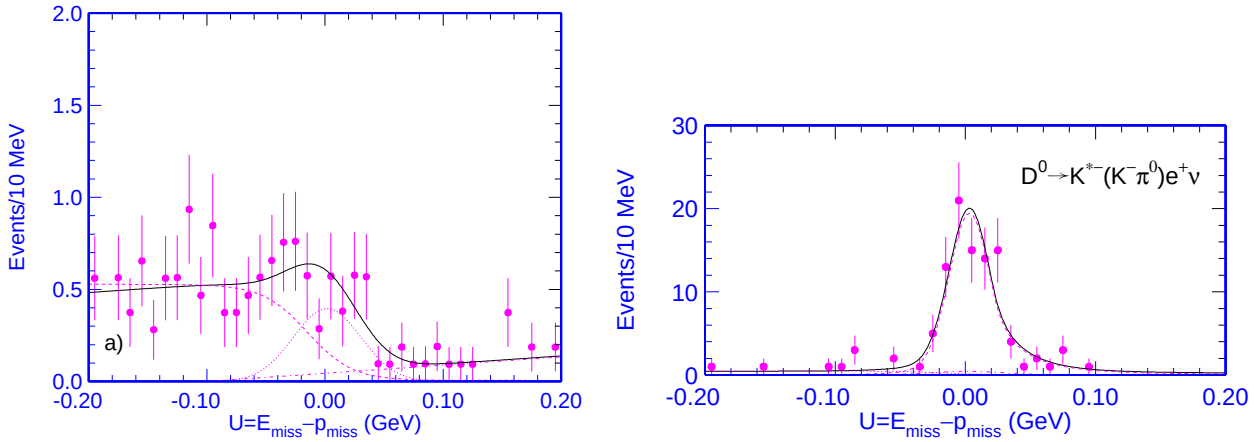

Figure 11: Fit to the backgrounds for $D^0 \to K^{*-}e^+\nu$ where $K^{*-} \to K^-\pi^0$ and fit to the U distribution, see text.

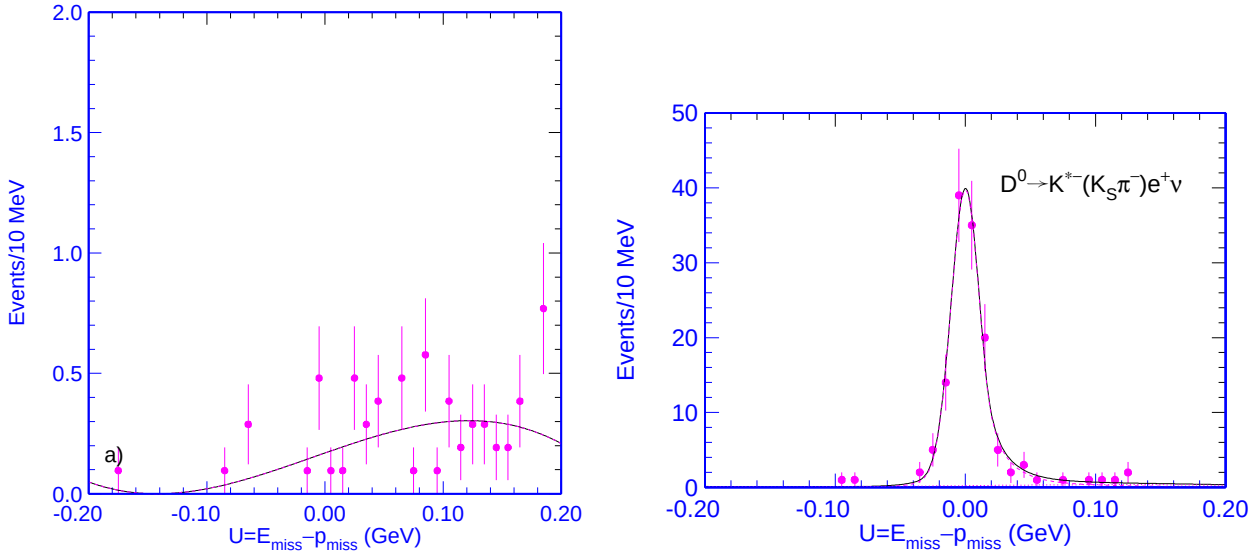

Figure 12: Fit to the backgrounds for $D^0 \to K^{*-}e^+\nu$ where $K^{*-} \to K_S\pi^-$ and fit to the U distribution, see text.

6.2 Results for $D^0 \to \rho^- e^+ \nu$

The comparison of U distribution between the data and MC for $D^0 \to \rho^- e^+ \nu$ is shown in Fig. 13 with different components of backgrounds. The fit to the backgrounds with a Gaussian for the dominant backgrounds from $D^0 \to K^{*-} e^+ \nu$ where $K^{*-} \to K^- \pi^0$ and a 2nd order polynomial is depicted in Fig. 14a. We fit the U distribution for the selected $D^0 \to \rho^- e^+ \nu$ events using a Gaussian plus Crystall Ball function (signal) and a Gaussian (background from $D^0 \to K^{*-} e^+ \nu$) plus a 2nd order polunomials with their shapes fixed at MC level, see Fig. 14b. The yield, efficiencies and branching fraction are given in Table 2.

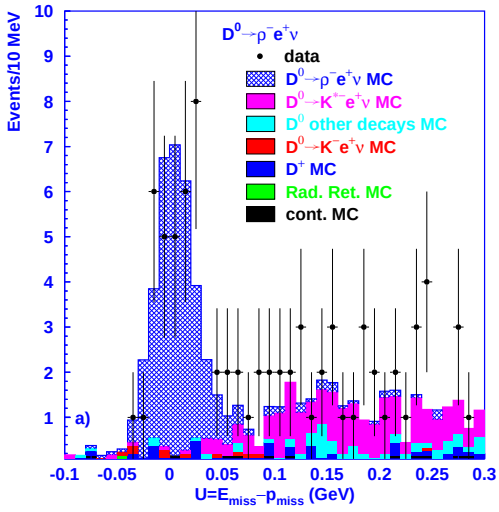

Figure 13: U distribution for the selected $D^0 \to \rho^- e^+ \nu$ events and the decomposition of backgrounds.

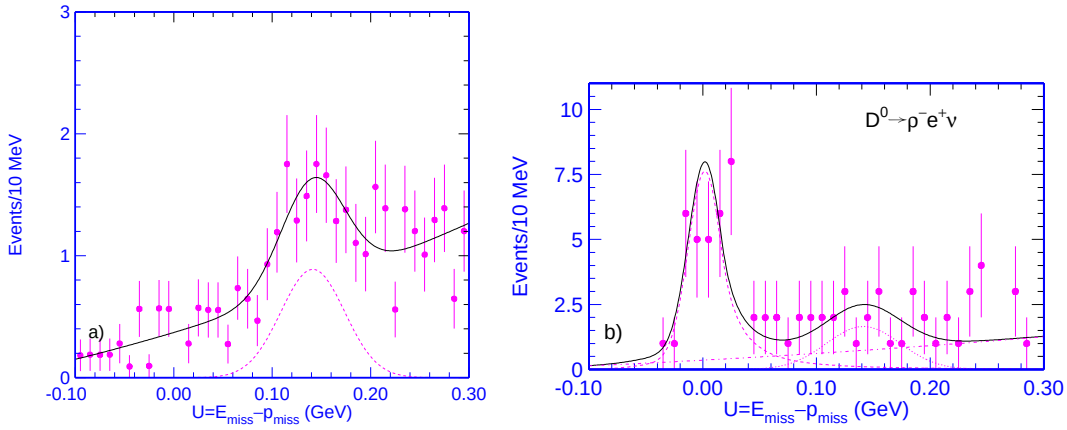

Figure 14: Fit to the backgrounds and fit to the U distribution for $D^0 \to \rho^- e^+ \nu$, see text.

7 Electron Identification Efficiency Correction

It is found that electron identification efficiency is 2.1% higher in MC than that in data. We correct the signal efficiencies and assign 1% systematics due to electron identification, see Chulsu's writeup [7].

In Table 2, we apply the electron identification efficiency correction to the efficiencies of reconstructing the D^0 semileptonic decays and the tag $\bar{D}^0$. Table 3 lists the branching fractions for $D^0 \to K^- e^+ \nu$ using different tag modes.

Table 2: Efficiencies for finding a tag $\bar{D}^0$ and D^0 semileptonic decays for $D^0 \to K^- e^+ \nu$, $D^0 \to \pi^- e^+ \nu$, $D^0 \to K^{*-} e^+ \nu$ and $D^0 \to \rho^- e^+ \nu$. The overall effective efficiencies for finding D^0 semileptonic decays are also given.

Signal Modes	$D^0 \to K^- e^+ \nu$	$\pi^- e^+ \nu$	$K^{*-}(K^-\pi^0)e^+\nu$	$K^{*-}(K_S\pi^-)e^+\nu$	$\rho^- e^+ \nu$
Tags	ϵ (%)	ϵ (%)	ϵ (%)	ϵ (%)	ϵ (%)
$K^-\pi^+$	41.89 ± 0.21	48.65 ± 0.21	14.60 ± 0.15	27.34 ± 0.17	18.48 ± 0.17
$K^-\pi^+\pi^0$	22.16 ± 0.18	25.70 ± 0.19	7.70 ± 0.11	13.68 ± 0.12	9.33 ± 0.12
$K^-\pi^+\pi^0\pi^0$	11.01 ± 0.13	12.85 ± 0.14	4.01 ± 0.08	6.68 ± 0.09	4.78 ± 0.09
$K^-\pi^+\pi^+\pi^-$	28.28 ± 0.19	33.08 ± 0.20	10.13 ± 0.13	17.66 ± 0.14	12.12 ± 0.14
$K_S\pi^+\pi^-$	23.90 ± 0.18	28.05 ± 0.19	8.60 ± 0.12	15.20 ± 0.13	10.45 ± 0.13
$K_S\pi^+\pi^-\pi^0$	12.94 ± 0.14	14.79 ± 0.15	4.46 ± 0.09	7.71 ± 0.10	5.32 ± 0.10
$K_S\pi^0$	21.43 ± 0.18	24.58 ± 0.18	7.41 ± 0.11	13.49 ± 0.12	9.19 ± 0.12
$\pi^-\pi^+\pi^0$	26.98 ± 0.19	31.06 ± 0.20	9.55 ± 0.13	16.69 ± 0.14	11.47 ± 0.14
K^-K^+	35.96 ± 0.21	41.29 ± 0.21	13.07 ± 0.14	23.44 ± 0.16	15.95 ± 0.16
overall ϵ	65.44±0.50	76.03±0.53	23.08±0.33	40.85±0.41	28.01±0.36
yields	1392.4±37.2	119.0±11.0	92.1±10.2	126.4±11.5	35.2±7.3
$\mathcal{B}(\times 10^{-3})$	(33.89±0.90)	2.49±0.23	19.32 ± 2.13	21.50 ± 1.95	2.03±0.42

8 Cross Checks

We also fit the U distributions with a double Gaussian for signals instead of a Gaussian and Crystall Ball function as a cross check. The fits are shown in Fig. 15. The fits result in a cutoff near 0.1 GeV, therefore with a bit lower efficiencies. The yields are 1368±38, 112.6±10.8, 91.0±9.3, 124.8 ± 10.8, 36.1±7.1 for $D^0 \to K^- e^+ \nu$, $D^0 \to \pi^- e^+ \nu$, $D^0 \to K^{*-} e^+ \nu$ with $K^{*-} \to K^- \pi^0$ and $K^{*-} \to K_S \pi^-$ and $D^0 \to \rho^- e^+ \nu$, respectively. The corresponding efficiencies are 2.1%, 4.5%, 1.5%, 1.4%, 3.0% lower. The relative differences of the efficiency corrected yields are

Table 3: $\mathcal{B}(D^0 \to K^-e^+\nu)$ with different tag modes.

tags: $D^0 \to$	yields	$\mathcal{B}(\%)$
$K^-\pi^+$	242.0 ± 15.6	3.73 ± 0.24
$K^-\pi^+\pi^0$	413.1 ± 20.5	3.34 ± 0.17
$K^-\pi^+\pi^0\pi^0$	107.5 ± 10.2	3.23 ± 0.34
$K^-\pi^+\pi^+\pi^-$	305.2 ± 18.7	3.25 ± 0.20
$K_S\pi^+\pi^-$	96.9 ± 10.1	3.17 ± 0.34
$K_S\pi^+\pi^-\pi^0$	115.5 ± 11.2	3.82 ± 0.41
$K_S\pi^0$	25.8 ± 5.2	2.47 ± 0.50
$\pi^-\pi^+\pi^0$	63.5 ± 8.1	3.53 ± 0.49
K^-K^+	21.3 ± 4.7	3.70 ± 0.83

-0.4%, $+1.0\%$, -0.3%, -0.1%, $+1.3\%$ for the above decay modes. It means two procedures give consistent results. Please note the efficiency differences using two signal PDFs is mode-dependent, it also depends on how fast the tail drops and how long the tail is.

We also use two procedures to determine the branching fraction for $D^0 \to K^-e^+\nu$ in the generic MC, and the obtained results are consistent with the input branching fractions.

9 Tests with Generic MC

9.1 Tests for D^0 Semileptonic Decays with Generic MC

We use generic MC sample (10 times our data sample) and follow our procedure to see what branching fractions for D^0 semileptonic decays we measure, and compare with the built-in branching fractions in the MC.

In Table 4, we present our measured branching fractions in generic MC, in comparison with those built in MC. We see that our measured branching fractions are in excellent agreement with those built in MC. That gives us strong confidence on our procedure which also gives higher efficiencies. Please note, no electron identification effciency correction applies when testing on generic MC.

9.2 Tests for $D^0 \to K^-e^+\nu$ with Generic MC

For $D^0 \to K^-e^+\nu$ with large statistics, we also measure tag-by-tag branching fractions in generic MC, our measured branching fractions shown in Table 5 are in good agreement with the built-in branching fraction 3.64%.

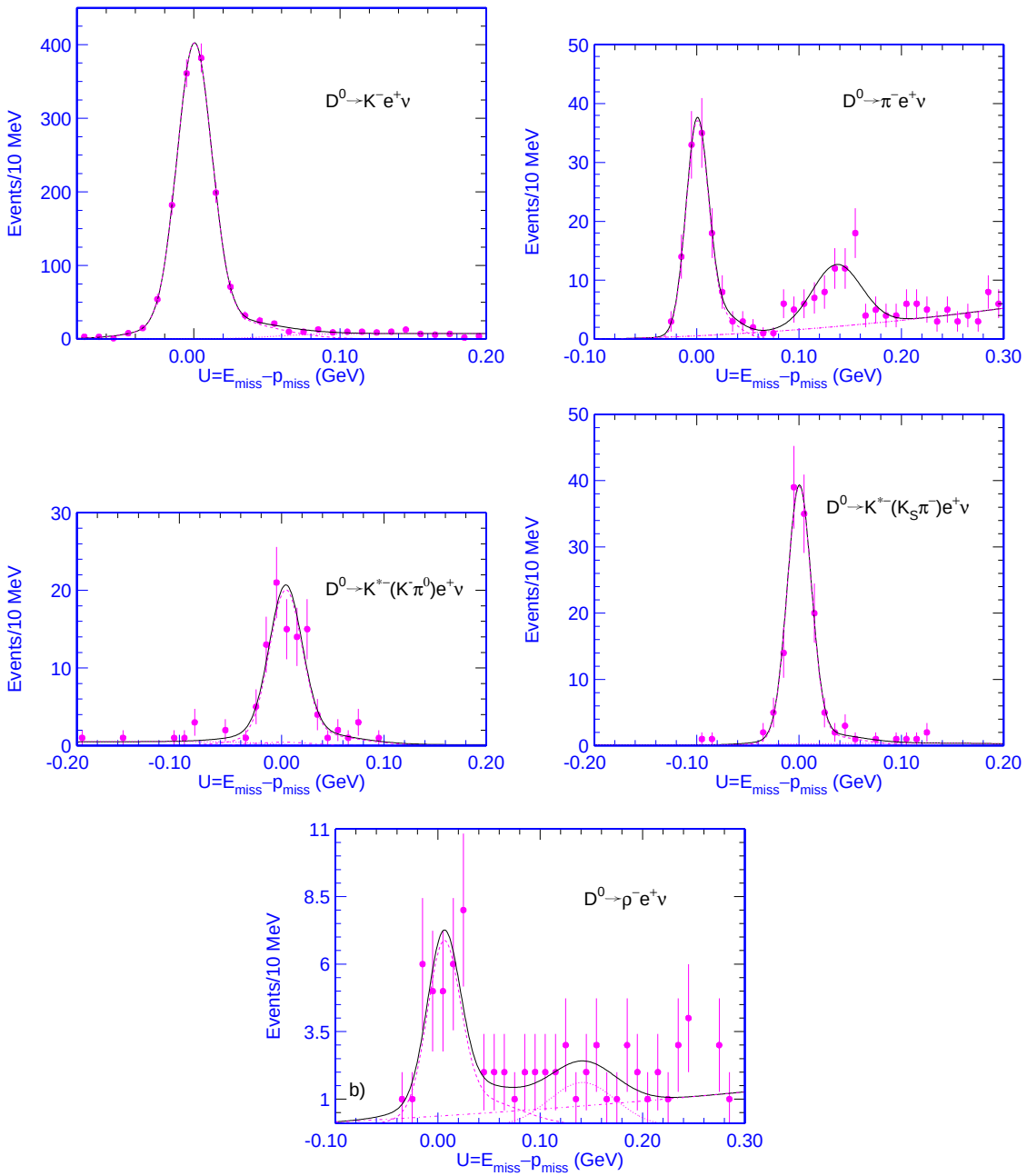

Figure 15: Fits to the U distributions for $D^0 \to K^- e^+ \nu$, $D^0 \to \pi^- e^+ \nu$, $D^0 \to K^{*-} e^+ \nu$ with $K^{*-} \to K^- \pi^0$ and $K^{*-} \to K_S \pi^-$, and $D^0 \to \rho^- e^+ \nu$ with a double Gaussian for signals instead of a Gaussian and Crystall Ball function. The fits result in a cutoff near 0.1 GeV.

Table 4: Measured branching fractions for the D^0 semileptonic decays in 10 times generic MC sample, in comparison with the built-in branching fractions.

modes	$\mathcal{B}$ in MC	Measured $\mathcal{B}$
$D^0 \to K^- e^+ \nu$	3.64%	$(3.62 \pm 0.03)\%$
$D^0 \to \pi^- e^+ \nu$	3.7×10^{-3}	$(3.65 \pm 0.09) \times 10^{-3}$
$D^0 \to K^{*-}(K_S\pi^-)e^+\nu$	2.02%	$(2.05 \pm 0.06)\%$
$D^0 \to K^{*-}(K^-\pi^0)e^+\nu$	2.02%	$(2.05 \pm 0.06)\%$
$D^0 \to \rho^- e^+ \nu$	2.9×10^{-3}	$(2.82 \pm 0.14) \times 10^{-3}$

Table 5: Measured branching fractions for $D^0 \to K^- e^+ \nu$ in 10 times generic MC sample with different tags, in comparison with the built-in branching fraction: 3.64%.

tags $D^0 \to$	Measured $\mathcal{B}(\%)$
$K^-\pi^+$	3.58 ± 0.07
$K^-\pi^+\pi^0$	3.57 ± 0.05
$K^-\pi^+\pi^0\pi^0$	3.61 ± 0.10
$K^-\pi^+\pi^+\pi^-$	3.68 ± 0.07
$K_S\pi^+\pi^-$	3.78 ± 0.12
$K_S\pi^+\pi^-\pi^0$	3.53 ± 0.12
$K_S\pi^0$	3.68 ± 0.20
$\pi^-\pi^+\pi^0$	3.61 ± 0.15
K^-K^+	3.58 ± 0.24

10 Systematics

We have considered the following sources of systematics which may affect the results: charged track, K_S and π^0 finding systematics, veto on the extra track, background shape, MC statistics, model-dependent form factors, hadron identification, electron identification. Their contributions to systematics are discussed as follows.

Systematics for track finding efficiency is 0.7% per charged track, 3.0% per K_S and 2.5% per π^0 by D hadron group [8]. MC statistics varies from 0.5% to 3%, depending on the tag modes, see Table 1 and 2. The electron identification efficiency uncertainty is 1% with efficiency correction applied from the study by Chulsu [7].

As discussed before, the extra tracks in an event is well modeled in our MC. Using the selected $D^0 \to K^- e^+ \nu$ events, we find 0.6% events have extra tracks in our data, 0.3% events in our MC. The data and MC agrees very well, the difference is less than 0.5%. We asign a 0.5% systematics due to the veto on extra tracks.

To estimate the systematics from the backgrounds, we vary the background functions (including potential peaking backgrounds for $D^0 \to K^{*-} e^+ \nu$ and $D^0 \to \rho^- e^+ \nu$) by $\pm 1\sigma$, taking the correlation of parameters into account. We find the background shape and possible peaking backgrounds for $D^0 \to K^{*-} e^+ \nu$ and $D^0 \to \rho^- e^+ \nu$ contributes a systematis of $< 1\%$, 1.6%, 2.5%, 1.5% and 5.0% for $D^0 \to K^- e^+ \nu$, $D^0 \to \pi^- e^+ \nu$, $D^0 \to K^{*-} e^+ \nu$ with $K^{*-} \to K^- \pi^0$ and $K^{*-} \to K_S \pi^-$ and $D^0 \to \rho^- e^+ \nu$, respectively.

When we select the D^0 semileptonic decays, we apply a cut on the beam constrained mass of the tag $\bar{D}^0$. We vary the cut, both signal yields and efficiencies vary a little, while the efficiency corrected yields vary by less than 0.6% for the above modes, and we assign a 0.6% systematics due to the cut on the beam constrained mass of the tag $\bar{D}^0$. It is mainly attributed to the differnces of the beam constrained mass resolutions in data and MC for the tag modes with one or more π^0's.

10.1 Model Dependent Systematis

We obtain the detection efficiencies based on ISGW2 model for D semileptonic decays. It is found that this model does not describe the data well. Our long term plan is that we will study the differential decay rate to extract the infomation of form factors. For the time being, we try to take advantage of our current knowledge of the form factors for D semileptonic decays. To estimate the systematics due to the model, we use the form factors from the analysis of $D^0 \to K^- e^+ \nu$ and $D^0 \to \pi^- e^+ \nu$ at CLEO III [9]. The fit to the differential decay rate to extract the information of form factors is dipicted in Fig. 16. We used the parameters given in Ref. [9] to generate signal MC and find the efficiencies vary less than 1% for $D^0 \to K^- e^+ \nu$ and $D^0 \to \pi^- e^+ \nu$.

For $D^0 \to K^{*-} e^+ \nu$ and $D^0 \to \rho^- e^+ \nu$, we use the parameterization of form factors from the study of $D^+ \to \bar{K}^{*0} e^+ \nu$ at E791 [10] to generate signal MC. The E791 analysis is shown in Fig. 17. We find that the efficiencies vary less than 1% for $D^0 \to K^{*-} e^+ \nu$ and 1.6% for $D^0 \to \rho^- e^+ \nu$, it

is suggested a conservative systematics of 3.0% be assigned for $D^0 \to \rho^- e^+ \nu$ by the committee.

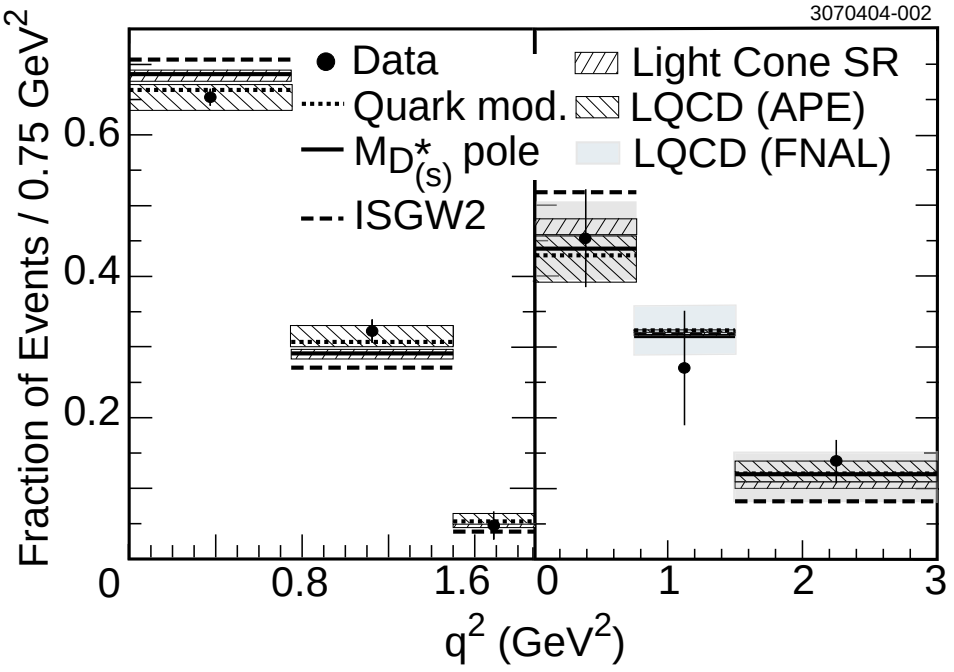

Figure 16: Analysis of differential decay rate to extract form factors for $D^0 \to K^- e^+ \nu$ and $D^0 \to \pi^- e^+ \nu$ at CLEO III [9].

10.2 Hadron Identification Systematics

Since the hadron momentum spectra from D semileptonic decays cover up to 1.1 GeV/c, we combine $D^0 \to K^-\pi^+$ and $D^+ \to K^-\pi^+\pi^+$ to study hadron identification efficiency in our data and MC. We require that the beam constrained masses for $D^0 \to K^-\pi^+$ and $D^+ \to K^-\pi^+\pi^+$ candidates must be within 5 MeV of their nominal masses, and $|\Delta E| < 20$ MeV, the ΔE sidebands within (45,65) MeV and (-65,-45) MeV are used to subtract the residual random combinational backgrounds. Since kinematics of the threshold production provide powerful means to reject backgrounds from misidentified and missing particles as discussed in Sect. 3.4. We use the following loose hadron identification criteria to obtain higher efficiency as discussed in Sect. 3.4:

- $3|\sigma|$ dE/dx for kaons and pions;
  for $p > 0.7$ GeV, $LL_\pi - LL_K + \sigma_\pi^2 - \sigma_K^2 > (<)0$ for K(π) within $|\cos\theta| < 0.8$ if RICH available (without cut on $N^\gamma_{K(\pi)}$); otherwise, $\sigma_\pi^2 - \sigma_K^2 > (<)0$ for kaons and pions.

In Fig. 18, we present momentum dependent kaon and pion identification efficiencies with the above requirements. The comparison shows good agreement between our data and MC and the difference is less that 0.2-0.3% for hadrons with p< 0.7 GeV/c. for pions with $p >$0.7 GeV/c, data and MC agree to less than 1% level, for kaons with $p > 0.7$ GeV/c, data and MC agree to about

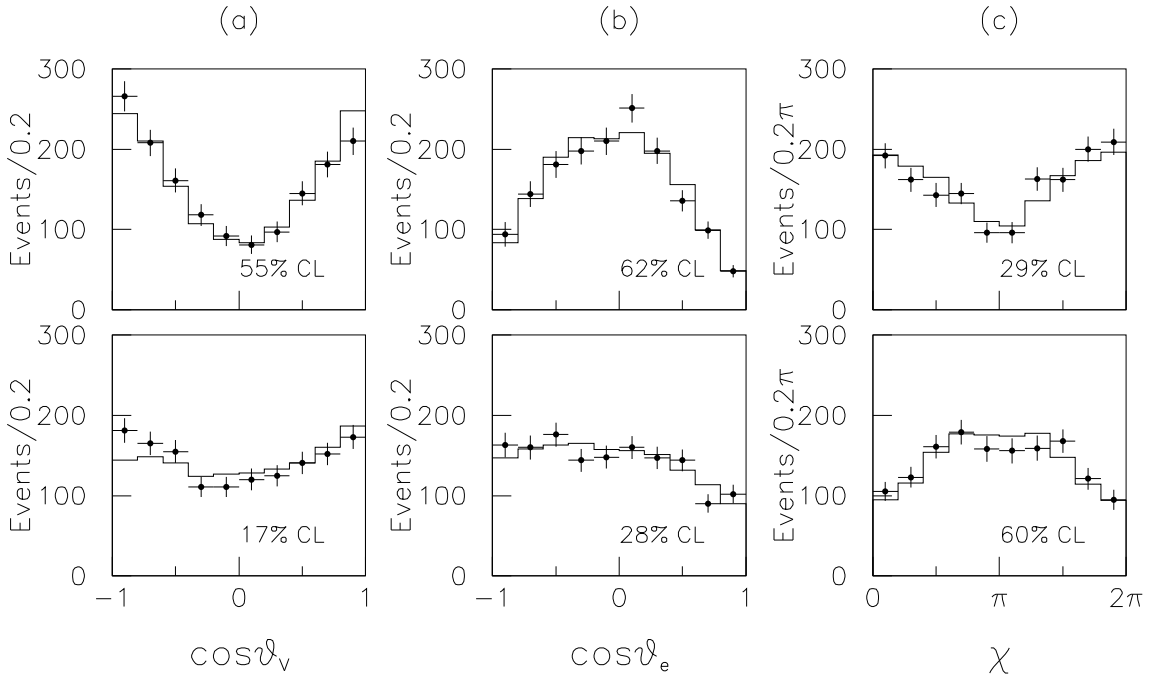

Figure 17: Analysis of $D^+ \to \bar{K}^{*0} e^+ \nu$ at E791 [10].

1.5% level. The overall difference is less than 1%. We assign a 1% systematics due to hadron identification.

10.3 Systematics

In addition to the systematic uncertaities described above, Purdue group also estimates some extra uncertainties [12]. The uncertainty in the tag yields is estimated by using different signal PDFs and found to be $\sqrt{(1.9^2 - 1.3^2)}\%$=1.4% since we let the E_{beam} float when fitting the beam constrained masses, we only have one systematics on the tag yields. The uncertainties from the non-resonant backgrounds are estimated to be 2.2% for $D^0 \to K^{*-}(K^-\pi^0)e^+\nu$ and $D^0 \to K^{*-}(K_S\pi^-)e^+\nu$, and 4.4% for $D^0 \to \rho^- e^+\nu$. An uncertainty of 1.5% in the reconstruction efficiency for $D^0 \to K^{*-}(K^-\pi^0)e^+\nu$ is attributed to possible presence of a S-wave contribution in the decay amplitude as observed by FOCUS [13]

In Table 6, we summarize the systematics discussed above. The systematics from MC statistics is weighted with tag yields. We add these sources in quadrature to obtain the total systematics for each decay mode. In our procedure to obtain the branching ratios (see Eq. (6)), tag D's appear in both the denominator and nominator for N_{tag} and N_{signal}, and for ϵ_{tag} and ϵ_{signal}, the systematics from tag D's cancels. When calculating the ratios of branching fractions, the common systematics cancel.

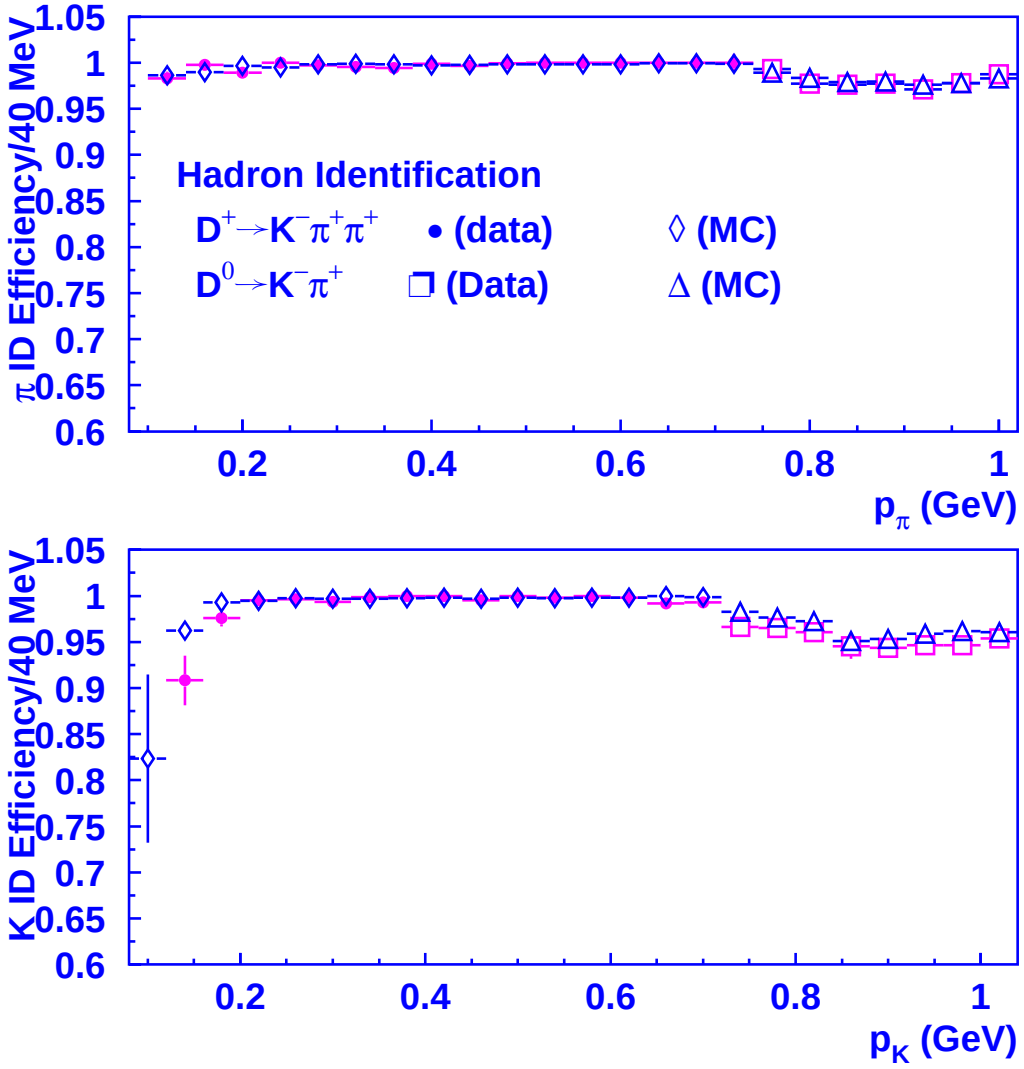

Figure 18: Comparison of kaon and pion identification efficiencies with the requirements described in the text.

Table 6: Systematics for four D^0 semileptonic decays (in %).

sources	$D^0 \to K^- e^+ \nu$	$\pi^- e^+ \nu$	$K^{*-}(K^-\pi^0)e^+\nu$	$K^{*-}(K_S\pi^-)e^+\nu$	$D^0 \to \rho^- e^+ \nu$
tracking	1.4	1.4	1.4	1.4	1.4
EID	1	1	1	1	1
PID	1	1	1	1	1
extra track	0.5	0.5	0.5	0.5	0.5
D^0 tag yields	1.4	1.4	1.4	1.4	1.4
M_{bc} cut	0.6	0.6	0.6	0.6	0.6
(common errors)	2.6	2.6	2.6	2.6	2.6
K_S finding	–	–	–	3.0%	–
π^0 finding	–	–	2.5	–	2.5
MC statistics	0.8	0.7	1.4	1.0	1.3
backgrounds	1	1.6	2.5	1.5	5.0
Form factors	<1	<1	<1	<1	3.0
nonresonant	–	–	2.2	2.2	4.4
S-wave	–	–	1.5	–	–
(subtotal)	1.6	2.0	4.7	4.3	7.8
total	3.0	3.3	5.4	5.0	8.2

11 Results

The branching fractions for D^0 exclusive semileptonic decays are listed in Table 7, we have improved measurements of the decay branching fractions for D^0 decays to $K^- e^+ \nu$, $\pi^- e^+ \nu$, $K^{*-} e^+ \nu$, and presented the first observation and measurement of $D^0 \to \rho^- e^+ \nu$.

Table 7: Branching ratios for five D^0 semileptonic decays.

Decays	$\mathcal{B}$	PDG
$D^0 \to K^- e^+ \nu$	$(3.39 \pm 0.09 \pm 0.10)\%$	$(3.58 \pm 0.18)\%$
$D^0 \to \pi^- e^+ \nu$	$(2.49 \pm 0.23 \pm 0.08) \times 10^{-3}$	$(3.6 \pm 0.6) \times 10^{-3}$
$D^0 \to K^{*-}(K^-\pi^0) e^+ \nu$	$(1.93 \pm 0.21 \pm 0.10)\%$	
$D^0 \to K^{*-}(K_S\pi^-) e^+ \nu$	$(2.15 \pm 0.20 \pm 0.11)\%$	
$D^0 \to K^{*-} e^+ \nu$ (combined)	$(2.05 \pm 0.14 \pm 0.08)\%$	$(2.15 \pm 0.35)\%$
$D^0 \to \rho^- e^+ \nu$	$(2.03 \pm 0.42 \pm 0.17) \times 10^{-3}$	none
$\frac{\mathcal{B}(D^0 \to \pi^- e^+ \nu)}{\mathcal{B}(D^0 \to K^- e^+ \nu)}$	$(7.4 \pm 0.7 \pm 0.2)\%$	$(10.1 \pm 1.8)\%$
$\frac{\mathcal{B}(D^0 \to \rho^- e^+ \nu)}{\mathcal{B}(D^0 \to K^{*-} e^+ \nu)}$	$(9.9 \pm 2.1 \pm 0.8)\%$	none

Our results for $D^0 \to K^- e^+ \nu$ and $D^0 \to K^{*-} e^+ \nu$ are consistent with those from the PDG. Our result $\mathcal{B}(D^0 \to \pi^- e^+ \nu)$ is lower than that from the PDG. The ratio $\frac{\mathcal{B}(D^0 \to \pi^- e^+ \nu)}{\mathcal{B}(D^0 \to K^- e^+ \nu)}$ is close to the CLEO III result $(8.2 \pm 0.6 \pm 0.5)\%$ [9], while lower than the PDG value. We have improved the measurements of these branching fractions. We expect better understanding of D semileptonic decays with much larger data sample in the near future at CLEO-c.

Acknowledgments

We'd like to thank our paper committee Ron A. Poling (chair), Werner Sun, Chulsu Park and Chaouki Boulahouache, our collaborators Victor Pavlunin and Ian Shipsey for their helpful suggestions and comments.

References

[1] Particle Data Group, K. Hagiwara *et al.*, Phys. Rev. D **66**, 010001 (2002). The update can be found at http://pdg.lbl.gov.

[2] CLEO-c Collaboration, CLNS-01/1742 (unpublished); J. D. Richman and P. R. Burchat, Reviews of Modern Physics, **67**, 893 (1995).

[3] R. Briere, CBX-04-32.

[4] D. Cassel *et al.*, CBX-04-38 and the update.

[5] F. Liu and Y. Gao, CBX-04-22.

[6] Modified Crystal Ball line shape is used to model this Gaussian core with a power-law tail due to the final state electron radiation:

$$f(x) = norm \begin{cases} e^{-\frac{(x-\bar{x})^2}{2\sigma^2}} & for\ \frac{x-\bar{x}}{\sigma} > -|\alpha|, \\ \frac{\left(\frac{n}{|\alpha|}\right)^n e^{-\frac{\alpha^2}{2}}}{\left(\frac{\bar{x}-x}{\sigma}+\frac{n}{|\alpha|}-|\alpha|\right)^n} & for\ \frac{x-\bar{x}}{\sigma} \leq -|\alpha|. \end{cases}$$

where α is the cross-over point from Gaussian to power-law in units of σ, n is real. The lower numbers of n give longer tails.

[7] Chulsu Park, http://www.lns.cornell.edu/~pcs/private/docs/meeting-lsl/20041129/main.pdf.

[8] D. Cassel *et al.*, CBX-04-39 and the update.

[9] G. S. Huang *et al.*, CLEO Collaboration, hep-ex/0407035, submitted to Phys. Rev. Lett..

[10] E.M. Aitala *et al.*, E791 Collaboration, Phys. Rev. Lett. **80**, 1393 (1998).

[11] D. Scora and N. Isgur, Phys. Rev. D **52**, 2783 (1995); N. Isgur *et al.*, Phys. Rev. D **39**, 799 (1989).

[12] V. Pavlunin and I. Shipsey, CBX-04-27.

[13] FOCUS Coll., J. M. Link *et al.*, Phys. Lett. B **535**, 43 (2002).